Phase switching in a system of two noisy Hodgkin-Huxley neurons coupled by a diffusive interaction

J. M. Casado*
Área de Física Teórica, Universidad de Sevilla, Apartado de Correos 1065, 41080 Sevilla, Spain

J. P. Baltanás†
Departamento de Matemáticas y Física Aplicadas y Ciencias de la Naturaleza, Universidad Rey Juan Carlos, c/ Tulipán s/n, 28933 Móstoles, Spain

(Received 9 June 2003; published 31 December 2003)

The focus of this paper is on the synchronous activity of a system of two intrinsically noisy Hodgkin-Huxley neurons coupled by a diffusive interaction. It is shown that conductance noise allows the relative phase of the neurons to display several different dynamical regimes ranging from phase and antiphase locking to random switching between two or more states. A synchronization diagram displaying the structure of the distribution function of the cyclic relative phase of the two neurons is presented. The addition of sinusoidal forcing terms to the equations governing the membrane voltage of both neurons gives rise to the statistical locking of those random switchings to the phase of the external signal.

DOI: 10.1103/PhysRevE.68.061917 PACS number(s): 87.10.+e, 87.16.−b, 05.40.−a

I. INTRODUCTION

Experimental evidence suggests that the synchronous activity of large assemblies of neurons provides the basis of the remarkable computational performance of the brain [1,2]. In an attempt to understand the origin and role of synchronous neuronal activity, a number of modeling approaches have been based on the description of each single neuron as a multidimensional oscillator [3]. Thus, the study of synchronization processes in ensembles of interacting nonlinear oscillators is basic for the understanding of some key issues in neuroscience. Most former theoretical investigations into the self-synchronization of ensembles of nonlinear oscillators have focused on the question to what extent the degree of synchronization can be controlled through the strength of the interoscillator coupling [4–7]. This formulation assumes that the synchronous activity of large neural systems is achieved through variation of synaptic interactions. However, it has been argued that transitions from desynchronized to synchronized states and vice versa could also be mediated by changes in the susceptibility of the neurons to external excitations [8]. From a theoretical point of view this idea implies that the interesting regime to model is the border between excitable and self-oscillatory behaviors of the neuron, a region where the internal noise of the cell could play a significant role as a promoter of neuronal synchronization.

The synchronization of two deterministic relaxation oscillators coupled by a diffusive interaction is a well known phenomenon. Some years ago, Sherman and Rinzel [9] observed dephasing and antiphase locking in simulations of two diffusively coupled neurons, while the effects of synaptic coupling, both of excitatory and inhibitory character, on the synchronization of neural firing were tackled by Vreeswijk *et al.* [10]. On the other hand, Hansel and co-workers [11] investigated the phase dynamics of two weakly coupled Hodgkin-Huxley (HH) neurons and showed the existence of out-of-phase locking between them. Later on, Han and co-workers [12] explained these results by investigating the dynamics of the relative phase of an ensemble of coupled Morris-Lecar neurons. The Morris-Lecar system [13] is a simplified version of the original Hodgkin-Huxley model of neuronal dynamics [14], in which the four variables of this last system have been reduced to only two without affecting in a drastic manner the qualitatively features of the original model. By restricting to the weak coupling limit, as their approach is valid as long as the shape of the limit cycle is only weakly altered by the interaction, Han and co-workers [12] showed that it is not immediately obvious whether the net result of diffusive coupling will lead to synchronization or desynchronization of two coupled oscillators. However, for many cycle limit systems, weak diffusive coupling will lock the neurons in a stable out-of-phase oscillation with a phase difference of π. If the coupling is not weak enough, a complex evolution of the phases with alternating periods of synchronous and asynchronous activity would appear.

Synchronization phenomena have been also investigated in nonlinear stochastic systems. There, the phase description has been found to be useful for the analysis of synchronization in many systems of biological relevance. A great deal of these investigations have been based on the classical approach to synchronization in the presence of additive noise carried out some years ago by Stratonovich [15]. Usually, the noise acting on the elements of an ensemble of neurons has been introduced by means of a fluctuating current that is delivered to the neuron either by the rest of the elements of the ensemble (thus resembling a fluctuating synaptic input) or directly from the external world (thus simulating the action of an experimenter) [3]. The analysis of the phenomenological stochastic bifurcations taking place in noisy Van der Pol–Bonhoeffer [16] and FitzHugh-Nagumo [17] oscillators driven by weak additive noise has shown that external and/or

*Electronic address: casado@us.es
†Electronic address: baltanas@escet.urjc.es

synaptic noises induce these systems to move along *stochastic limit cycles* in a range of parameters where the deterministic equations do not show limit cycle behavior at all. Thus, additive noise decreases the effective threshold for firing and allows a weak interneuronal coupling to drive the neurons to synchrony [18].

In this paper, the effects of a different kind of noise will be investigated. Basic to our present understanding of the nervous system is the fact that the dynamics of ion channels underlies all the electrochemical phenomena taking place in nerve cells. Thus, central to the study of neuronal excitability is the connection between the microscopic properties of ion channels and the macroscopic behavior of nerve membranes. Following the development of patch-clamp techniques, which allowed to measure ion currents through individual ion channels for the first time [19], a number of numerical studies have been devoted to relate the stochastic behavior of individual ion channels to macroscopic currents that change in a highly deterministic manner [20]. More recently, some work has been carried out aiming to incorporate the stochastic description of ion channels into the framework of the Hodgkin-Huxley model of spiking dynamics. Chow and White, for example [21], have derived an analytical expression for the probability of spontaneous firing in analogy with a classical barrier-crossing problem and, under the assumption that sodium inactivation takes place at a much faster time scale than changes in the other variables appearing in the HH model, they have been able to incorporate a fluctuating term to the equation governing the sodium conductance in this model. On the other hand, Fox and Lu [22] have approached the problem starting from a master equation governing the stochastic dynamics of a large population of ion channels. This formulation allows these authors to contract the description of the dynamics to yield Langevin equations describing voltage-dependent fluctuations in the gate variables that account for the activation and inactivation of sodium channels and the activation of potassium channels.

In what follows, we will use the stochastic HH neuron model of Fox and Lu to investigate the synchronizing behavior of a pair of noisy neurons when the coupling as well as the noise intensity are varied. In particular, we are interested in the phase locking of these neurons when conductance noise is allowed to excite them from the resting state to a regime of random spiking. Regimes of phase and antiphase synchronization, as well as multistate phase dynamics have been found.

The forcing of the system by an external sinusoidal signal added to the equations for the membrane voltages allows us to lock this switching to the period of the forcing. This seems to be an interesting feature of the system's dynamics because, unlike what occurs in the usual stochastic resonance (SR) phenomenology, the variable that performs the well-to-well hoping motion does not appear explicitly in the Langevin description of the fluctuating dynamics.

II. THE HODGKIN-HUXLEY MODEL WITH CONDUCTANCE NOISE

Let us consider briefly the description of the space-clamped dynamics of a patch of neuronal membrane developed in the classic paper of Hodgkin and Huxley [14]. There, the temporal evolution of the voltage across the neuron's membrane $V(t)$ is governed by a differential equation of the form

$$C\frac{dV}{dt} = -g_{Na}^{*}m^{3}h(V-V_{Na}) - g_{K}^{*}n^{4}(V-V_{K}) - g_{L}(V-V_{L}) + I, \tag{1}$$

where $C=1\ \mu\mathrm{F/cm^2}$ is the capacitance per unit area of the membrane, and $g_{Na}^{*}=120\ \mathrm{mS/cm^2}$ and $g_{K}^{*}=36\ \mathrm{mS/cm^2}$ are the maximal conductances per unit area associated with sodium and potassium channels. The constants $g_L=0.3\ \mathrm{mS/cm^2}$ and $V_L=-54.4\ \mathrm{mV}$ are, respectively, the constant conductance per unit area and reversal potential associated with the leakage of ions through the membrane. Moreover, $V_{\mathrm{Na}}=50\ \mathrm{mV}$ and $V_K=-77\ \mathrm{mV}$ are the reversal potentials associated with the equilibrium distribution of Na^{+} and K^{+} ions across the axonal membrane [14]. The constant I represents a stimulus or constant (tonic) current that is delivered externally to the neuron. The adimensional gate variables $m(t), h(t)$, and $n(t)$ that govern the activation and inactivation of sodium channels and the activation of potassium channels, respectively, obey the following set of differential equations:

$$\frac{dm}{dt} = \alpha_m(V)(1-m) - \beta_m(V)m,$$

$$\frac{dh}{dt} = \alpha_h(V)(1-h) - \beta_h(V)h,$$

$$\frac{dn}{dt} = \alpha_n(V)(1-n) - \beta_n(V)n, \tag{2}$$

where the experimentally determined voltage transition rates are given explicitly by the expressions [14]

$$\alpha_m(V) = \frac{0.1(V+40)}{1-\exp[-(V+40)/10]},$$

$$\beta_m(V) = 4\exp[-(V+65)/18],$$

$$\alpha_h(V) = 0.07\exp[-(V+65)/20],$$

$$\beta_h(V) = \{1+\exp[-(V+35)/10]\}^{-1},$$

$$\alpha_n(V) = \frac{0.01(V+55)}{1-\exp[-(V+55)/10]},$$

$$\beta_n(V) = 0.125\exp[-(V+65)/80]. \tag{3}$$

It can be shown [23] that, with this parametrization, the birth of limit cycles occurs at $I=I_{b1}\approx 6\ \mu\mathrm{A/cm^2}$ due to a saddle-node bifurcation of periodic orbits. On the other hand, the unstable branch of the periodic solutions dies at $I=I_{b2}\approx 9.8\ \mu\mathrm{A/cm^2}$ through an inverse Hopf bifurcation. Thus, in the parameter region $I<I_{b1}$, the resting state V_{rest}

≈ -65 mV is a globally stable solution whereas for $I_{b1} < I < I_{b2}$ the system has two stable attractors, a fixed point and a limit cycle. The focus of this work is on the parameter region near the onset of the saddle-node bifurcation of periodic orbits. In this *excitable region*, neurons are unable to fire spontaneously in the absence of noise.

A great deal of work has been devoted to study the effects of forcing on the HH model [23,24]. This has been done so far by allowing I to become a function of time of the general form

$$I = I_0 + I_{ext}(t) + I_{syn}(t), \tag{4}$$

where I_0 is a constant, $I_{ext}(t)$ is an external signal of deterministic or stochastic nature, and $I_{syn}(t)$ is a stochastic process that simulates the synaptic noise. In the case of a stochastic driving (and $I_0 < I_{b1}$) the HH system either fluctuates around the fixed point or makes large excursions around the limit cycle [24]. Thus, a source of additive noise in Eq. (1) induces voltage oscillations that appear as a train of spikes occurring at random times.

In this paper we are interested in describing the effects of conductance noise on the dynamics of the HH model. By conductance noise it is meant that we explicitly take into account the spontaneous fluctuations of the membrane conductance due to the intrinsically stochastic dynamics of the individual channels. As a consequence, and unlike the fluctuating terms appearing in Eq. (4), the conductance noise is an *intrinsic* property of each neuron. To model this kind of noise, we recall the stochastic HH model of Fox and Lu [22], where the voltage variable still obeys Eq. (1) but the gate variables are random quantities obeying the set of stochastic differential equations

$$\frac{dm}{dt} = \alpha_m(V)(1-m) - \beta_m(V)m + \xi_m(t),$$

$$\frac{dh}{dt} = \alpha_h(V)(1-h) - \beta_h(V)h + \xi_h(t),$$

$$\frac{dn}{dt} = \alpha_n(V)(1-n) - \beta_n(V)n + \xi_n(t), \tag{5}$$

where the noise terms $\xi_m(t)$, $\xi_h(t)$, and $\xi_n(t)$ are independent, zero-mean, Gaussian stochastic processes with autocorrelation functions given by [22]

$$\langle \xi_m(t)\xi_m(s)\rangle = \frac{D_{Na}\alpha_m\beta_m}{(\alpha_m+\beta_m)}\delta(t-s),$$

$$\langle \xi_h(t)\xi_h(s)\rangle = \frac{D_{Na}\alpha_h\beta_h}{(\alpha_h+\beta_h)}\delta(t-s),$$

$$\langle \xi_n(t)\xi_n(s)\rangle = \frac{D_K\alpha_n\beta_n}{(\alpha_n+\beta_n)}\delta(t-s). \tag{6}$$

The adimensional parameters D_{Na} and D_K are associated with the inverse of the total number of sodium and potassium channels present in a given patch of membrane. In order to reduce the number of parameters, and taking into account the number of sodium and potassium channels in a patch of membrane (60 potassium and 18 sodium channels per square micrometer [25]), we have taken $D_{\mathrm{Na}} = D$ and $D_{\mathrm{K}} = D/0.33$ so that the correct proportion between sodium and potassium channel densities is preserved.

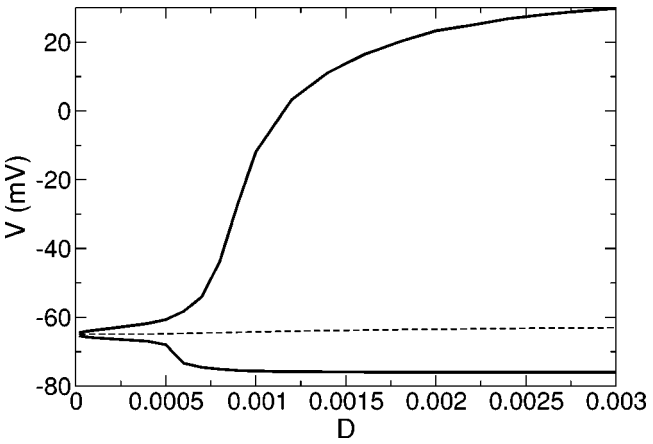

FIG. 1. Stochastic bifurcation diagram for the HH model with conductance noise when $I=0$. Notice that D is an adimensional parameter. Thick lines correspond to the top and bottom boundaries of the stationary distribution function of the membrane potential, $p_s(V)$. The dashed line stands for the mean value of the membrane potential computed over this distribution

As is well known, qualitative changes in the behavior of stochastic systems due to the modification of a parameter are termed phenomenological stochastic bifurcations. These bifurcations refer to qualitative changes in the stationary distribution of the variables. A typical feature that has been used to mark the occurrence of such a bifurcation is the number of modes of the stationary distribution function. The analysis of the stochastic bifurcation leading to spiking in the HH model subjected to a subthreshold tonic current plus additive synaptic noise has been carried out by Tanabe and co-workers [24]. Here, we show that a similar behavior takes place when the HH model is subjected to conductance noise.

The stationary distribution of the voltage is defined as the marginal probability distribution of the process $V(t)$,

$$p_s(V) = \int_0^1 dm \int_0^1 dh \int_0^1 dn\, p_s(V,m,h,n), \tag{7}$$

where $p_s(V,m,h,n)$ is the time average of the joint probability distribution $p(V,m,h,n;t)$ of the random processes $V(t), m(t), h(t)$, and $n(t)$ that define the stochastic HH model

$$p_s(V,m,h,n) = \lim_{T\to\infty}\frac{1}{T}\int_0^T dt\, p(V,m,h,n;t). \tag{8}$$

Histograms representing the marginal stationary distribution for the membrane voltage $p_s(V)$ have been determined from the numerical simulation of the stochastic system by using the algorithm put forward in Ref. [28]. In Fig. 1, we present the bifurcation diagram obtained from these histograms. The

thick lines appearing in this diagram are the top and bottom boundaries of the stationary distribution function of the membrane potential $p_s(V)$ as functions of the noise intensity D. These boundary lines have been drawn so that 1% of p_s is beyond the top line and another 1% is below the bottom one.

At low noise ($D<0.0005$), the voltage $V(t)$ performs small random oscillations around the resting state of the system. In this regime, the stochastic bifurcation diagram reminds one of the ''canard'' zone that appears close to the Hopf bifurcation threshold in the FitzHugh–Nagumo model [26]. This small-amplitude oscillatory behavior corresponds to the silent regime of the neuron because no spikes are produced, and is characterized by a nearly Gaussian $p_s(V)$. As the noise is increased, the system is driven to fire randomly, and a second mode of $p_s(V)$ appears at high values of V that is associated with the performing of large excursions of the system variables through the phase space. This change in the structure of $p_s(V)$ as D changes can be associated with the occurrence of a phenomenological stochastic bifurcation. As we can notice in Fig. 1, and in contrast with what occur at a deterministic bifurcation, the transition from one stationary distribution to another qualitatively different one proceeds progressively when the bifurcation parameter is varied.

On the other hand, as suggested by the results shown in a previous study [27], the mean firing rate of an isolated Hodgkin-Huxley neuron with fluctuating conductances increases with increasing noise level for every value of the current $I<I_{b1}$. Thus, conductance noise shifts the onset of oscillatory behavior to lower values of I, thus cooperating with the coupling to synchronize the neurons. This is the basis of the noise-induced frequency locking between neurons.

III. NOISE-INDUCED PHASE SWITCHING

Let us consider a system composed by two Hodgkin-Huxley neurons coupled to each other by a diffusive interaction. The equations of this system explicitly read

$$\begin{aligned} C\frac{dV_1}{dt} &= -g_{Na}^{*}m_1^3h_1(V_1-V_{Na})-g_K^{*}n_1^4(V_1-V_K)-g_L(V_1 \\ &\quad -V_L)+\epsilon(V_1-V_2)+I_1, \\ C\frac{dV_2}{dt} &= -g_{Na}^{*}m_2^3h_2(V_2-V_{Na})-g_K^{*}n_2^4(V_2-V_K)-g_L(V_2 \\ &\quad -V_L)+\epsilon(V_2-V_1)+I_2, \end{aligned} \tag{9}$$

where $V_1(t)$ and $V_2(t)$ are the instantaneous voltages across the respective membranes of the two neurons and I_1 and I_2 are two constants. The parameter ϵ is the strength of the ''diffusive'' [12] or ''electrical'' [3] coupling between the neurons and can be interpreted as the conductance of the (symmetric) synaptic connections between them. Again, the gate variables of the two subsystems obey Eqs. (5).

The numerical integration of the resulting set of eight stochastic differential equations has been carried out by using a stochastic integration scheme with a step size $h=0.01$ [28]. In order to confine the conductances within the physically allowed values ranging from zero to g^* we have implemented numerically the procedure to make $m(t),h(t)$, and $n(t)$ always located between zero and one [22]. Next, two point processes of the form

$$z(t)=\sum_{n=1}^{N}\delta(t-t_n) \tag{10}$$

have been extracted from the crossing of the stochastic signals $V_1(t)$ and $V_2(t)$ through a predetermined threshold. Up strokes of the voltage variables are counted as spikes when they reach a minimum amplitude of 10 mV having previously crossed the reset value of -50 mV from below. This spike detection scheme discards any very rapid recrossing of the threshold at 10 mV, an effect that increases in probability as the noise intensity is increased. Each one of the aforementioned point processes gives the temporal sequence of spike occurrences $\{t_n\}$ for a particular neuron.

Let us consider two identical neurons with $I_{1(2)}=6\ \mu\mathrm{A/cm}^2$. For this value of the tonic current the neuron is in the so-called *excitable regime*, where the deterministic attractor is the rest state and the firing can be excited by the noise. In what follows, we will consider the strength of noise acting on both neurons to be identical, $D_1=D_2=D$.

To study phase synchronization, we have associated a phase to the spike sequence $\{t_n\}$ of each neuron by means of the prescription [1]

$$\phi(t)=2\pi\frac{t-t_n}{t_{n+1}-t_n}+2\pi n, \quad t_n\leqslant t\leqslant t_{n+1}. \tag{11}$$

The phase synchronization of two neurons can be studied with reference to the instantaneous phase difference between them, $\psi(t)=\phi_1(t)-\phi_2(t)$. In stochastic systems this quantity is generally not constant even when the oscillators are frequency locked. For small coupling and/or strong noise intensity $\psi(t)$ will grow unbounded. However, if the coupling is increased and the noise level is not too high the relative phase will fluctuate around some constant level. At times, these stationary fluctuations will lead to a phase slip where the relative phase changes abruptly by $\pm 2\pi$. Thus, it is useful to define the phase locking condition in a statistical sense by using the cyclic relative phase

$$\Phi=\psi \pmod{2\pi}. \tag{12}$$

A dominant peak of the distribution of this cyclic relative phase $P(\Phi)$ will announce the existence of a preferred relative phase associated with the dynamical evolution of both neurons. When this preferred phase is zero we speak of phase synchronization in a statistical sense. Analogously, we can speak of out-of-phase synchronization when the distribution $P(\Phi)$ peaks around a nonzero value of Φ.

For the system at hand, a synchronization diagram in terms of the parameters ϵ and D has been obtained. This diagram, which is depicted in Fig. 2, presents several regions, each one characterized by a different form of the probability distribution $P(\Phi)$. The characteristic features of

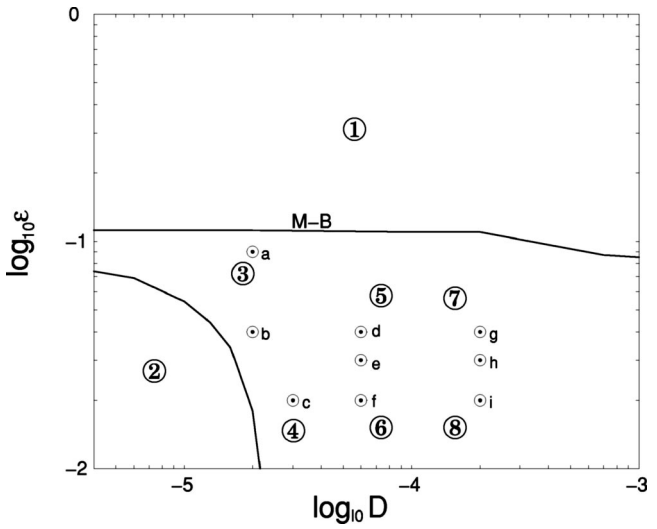

FIG. 2. Synchronization diagram for the relative phase of two noisy Hodgkin-Huxley neurons. Region 1 corresponds to states of statistical antiphase synchronization. In region 2 there is no noise-induced firing. The $M-B$ line corresponds to a function $\epsilon_0(D)$ giving the minimum value of the coupling strength ϵ for which a statistical phase locking is stable. D is the noise strength as it appears in Eq. (6) and the subsequent paragraph. Drifting behavior of the relative phase corresponds to the lower right corner of the diagram.

some distributions corresponding to the several regions appearing in the synchronization diagram are plotted in Figs. 3 and 6.

In region 1 of Fig. 2, the distribution $P(\Phi)$ shows a monomodal character and its peak is centered on $\psi=\pi$. Thus, this region corresponds to the antiphase locking state that appears at strong diffusive coupling. In our system there appears a minimum value of the coupling parameter ϵ_0 for which the antiphase locking becomes stable in a statistical sense. Furthermore, as we can observe in the synchronization diagram, this minimum coupling is quite independent of the noise intensity, as least for $D<2\times10^{-3}$. For large values of ϵ with respect to ϵ_0 the probability of the relative phase becomes rather narrow, thus indicating that for strong coupling the state of statistical antiphase synchronization is close to the full antiphase synchronization appearing in deterministic systems. An example of this kind of probability distribution is depicted in Fig. 3(a), whereas in Fig. 4(a) a realization of the process $\psi(t)$ for the same values of ϵ and D is depicted to show the fluctuating character of its temporal evolution. Indeed, the particular value of the base line around which the fluctuations are performed could be π or $-\pi$ depending of the realization. When ϵ is decreased and the line $M-B$ is approached the distribution function $P(\Phi)$ broadens. It also broadens if we move to higher noise intensities by keeping $\epsilon>\epsilon_0$ constant.

The crossing from above of the line $M-B$ corresponds to the distribution $P(\Phi)$ becoming bimodal. Just under this line the two peaks of the distribution are closely spaced but as ϵ is further decreased, these two peaks shift away and narrow. This focusing clearly reflects the two-state character of the phase dynamics. In Figs. 3(b) and 3(c) we depict the form of

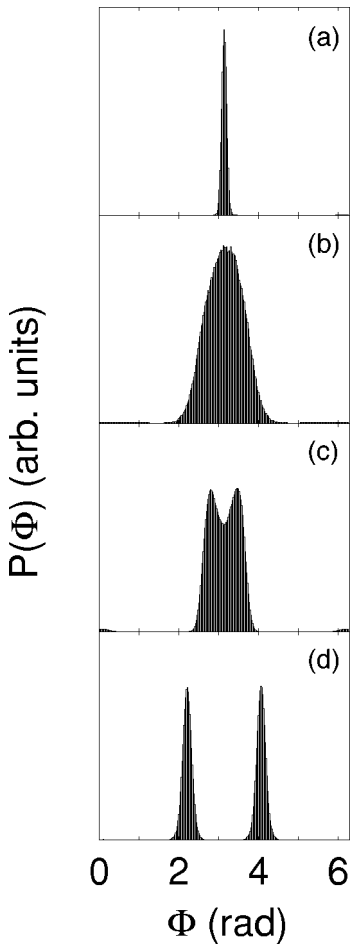

FIG. 3. Probability distribution of the cyclic relative phase for some characteristic values of coupling and noise. *A*, $\epsilon=0.16$; *B*, $\epsilon=0.12$; *C*, $\epsilon=0.11$; and *D*, $\epsilon=0.07$. In all cases $D=10^{-5}$. The panels have different vertical scales.

the distribution functions $P(\Phi)$ corresponding to values of ϵ located at both sides of the line $M-B$. The temporal evolution of some realizations of the stochastic process $\psi(t)$ corresponding to those cases appears in Fig. 4(b) and 4(c). In Fig. 3(d), on the other hand, the structure of $P(\Phi)$ for a

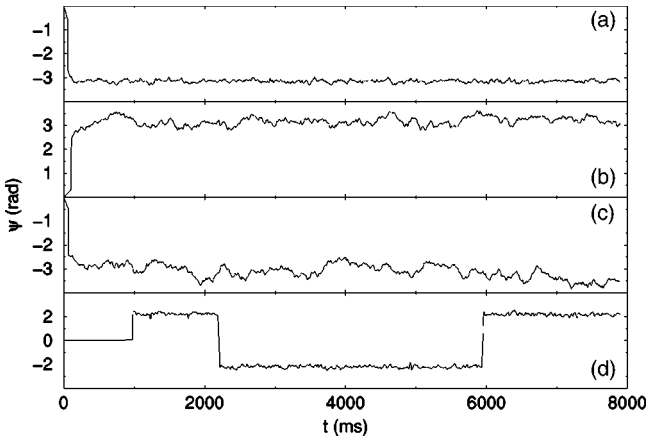

FIG. 4. A single realization of the stochastic process $\psi(t)$ corresponding to the four representative cases depicted in Fig. 3.

range of parameters well below the dividing line is shown. Its bimodal character neatly announces the main features of the phase evolution shown in Fig. 4(d). As we can observe in this last plot, the relative phase of both neurons fluctuates successively around a pair of symmetric values and, from time to time, jumps from one of them to the other take place. This two-state dynamics reflects a compromise between the effects of coupling and noise. Our findings thus imply that the relative phase of the system carries out a process of noise-induced phase switching between two symmetrical states resulting from the combined action of noise and coupling.

As a consequence, the fluctuating dynamics of the relative phase ψ in the region close to the line $M-B$ resembles the overdamped evolution of the coordinate of a particle in a one-dimensional double-well potential. In other words, we can characterize the temporal dependence of the relative phase by the stochastic differential equation

$$\dot{\psi} = -U'_{eff}(\psi) + \xi(t), \tag{13}$$

where $\xi(t)$ is some stochastic process that plays the role of a noise and U'_{eff} is the first derivative of an effective potential function $U_{eff}(\psi)$ that presents a single minimum if $\epsilon \leqslant \epsilon_0$ and two symmetric minima when $\epsilon > \epsilon_0$. Notice, however, that in the present situation the potential U_{eff} is not given *a priori*, as is the case in the usual setting of the Langevin description of fluctuations. In our case, the properties of this function depend on the dynamical behavior of a completely different system, namely, the system of differential equations describing the two neurons. Thus, the description of the dynamics of the relative phase provided by Eq. (13) can be considered only as a useful way of thinking.

In this context, we can say that a new phenomenological stochastic bifurcation takes place for the relative phase as the coupling parameter crosses the line $M-B$ in the synchronization diagram. As is customary in these cases, we plot a bifurcation diagram depicting the maxima Φ_{peak} of $P(\Phi)$ as the coupling parameter ϵ is varied. Such a diagram is presented in Fig. 5 for $D=10^{-5}$.

Region 2 in Fig. 2 corresponds to the silent state of both neurons. There, the combination of coupling and noise is unable to excite the firing and so, both neurons only perform low amplitude fluctuations around its resting potentials. On the other hand, the dynamics of the relative phase in region 3 corresponds to the bimodal structure of $P(\Phi)$ depicted in Figs. 3(c) and 3(d). As we approach region 2 from above, the peaks of this distribution shift to $\Phi=0=2\pi$. In region 5, on the other hand, the structure of $P(\Phi)$ has a complex multimodal character with two symmetrical peaks around $\Phi=\pi$, two extra peaks at $\Phi\approx 0$ and $\Phi\approx 2\pi$, and a number of smaller maxima. As we move towards smaller values of the coupling parameter, these two central peaks decrease in height and eventually disappear as we enter region 6. This last region is thus characterized by a bimodal distribution with peaks centered around π and 0. In region 4, on the other hand, the peak around π also disappears. In region 7, the distributions are again of a bimodal character but they have smaller wings than those of region 5. As we decrease

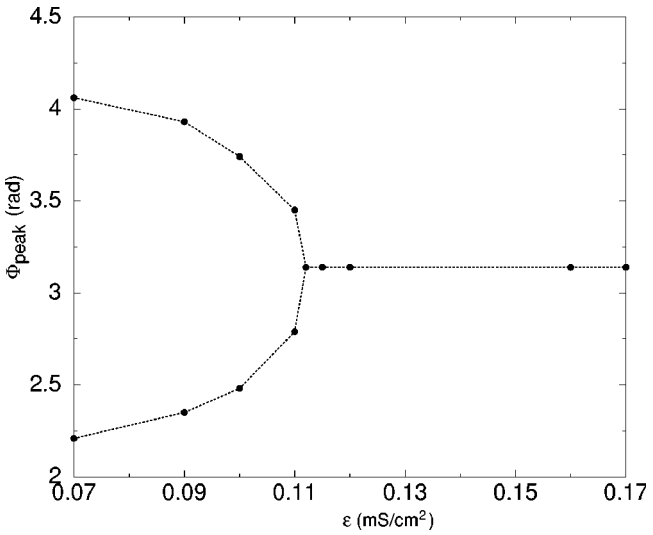

FIG. 5. Bifurcation diagram showing the maxima of $P(\Phi)$ as functions of the coupling strength ϵ for $D=10^{-5}$. Points correspond to the results of the simulation and the dotted line appears only as a guide to the eye.

the coupling parameter ϵ, we enter region 8 where the structure of the distribution function $P(\Phi)$ is monomodal with highly developed wings. The drifting behavior of the relative phase corresponds to the lower right corner of the diagram. In this synchronization diagram no lines have been plotted separating the aforementioned regions because the structure of $P(\Phi)$ changes in a continuous manner when we move either ϵ or D and it will be rather arbitrary to draw separation lines among regions of closely related behavior. In Fig. 6 we have plotted some representative distribution functions corresponding to different combinations of ϵ and D. Isolated points marked in the synchronization diagram correspond to

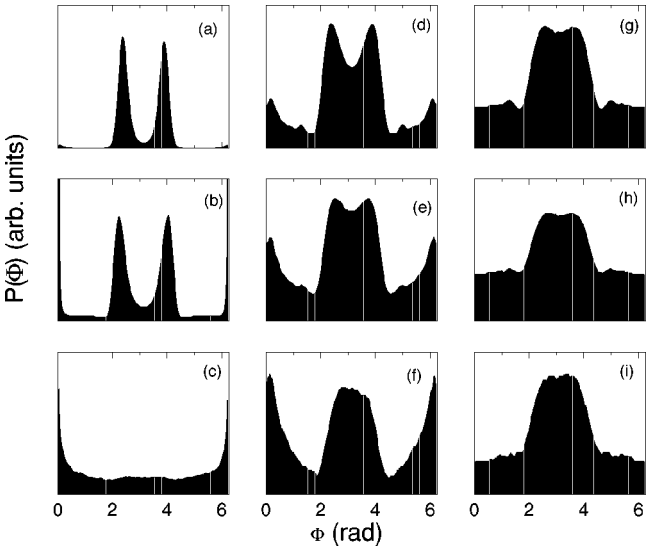

FIG. 6. The distributions of the cyclic relative phase $P(\Phi)$ corresponding to some representative points of the synchronization diagram specified in Fig. 2. Typically, each one of these distributions has been plotted by using 10^3 stochastic realizations of Φ, each one lasting 8 s.

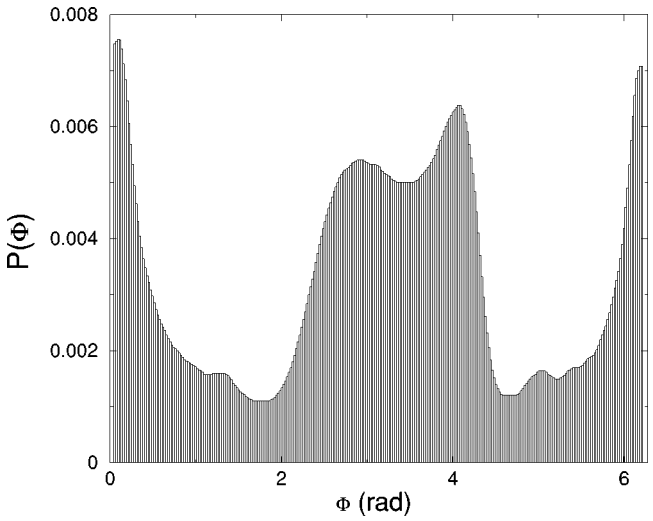

FIG. 7. The distribution of the cyclic relative phase corresponding to the point *d* in the synchronization diagram ($\epsilon=0.04$, $D=6\times10^{-5}$) for an asymmetrical system in which the tonic signal acting on neuron 1 was $I_1=6\ \mu\mathrm{A/cm}^2$ while that corresponding to neuron 2 was $I_2=5\ \mu\mathrm{A/cm}^2$.

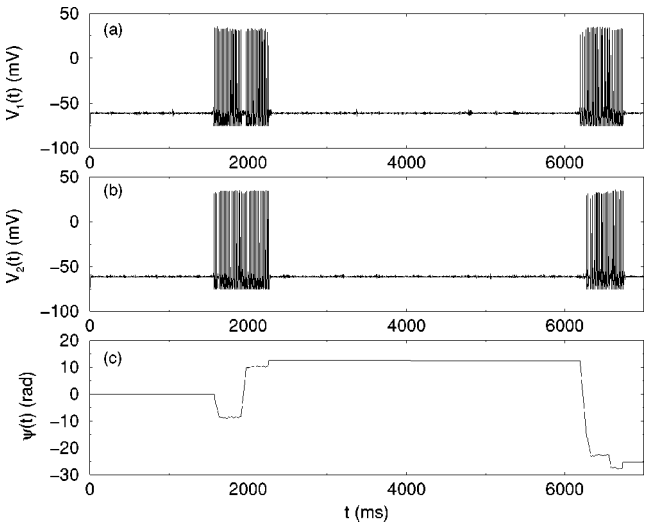

FIG. 8. Bursting behavior for $\epsilon=0.03$ and $D=2\times10^{-5}$. In panels (a) and (b) two single realizations of the membrane potentials V_1 and V_2 are depicted. In panel (c) we can observe the temporal evolution of the relative phase $\psi(t)$ corresponding to these particular realizations. The distribution of the cyclic relative phase $P(\Phi)$ corresponding to this case belongs to region 4 in Fig. 2.

the different distributions depicted in this last figure.

The structure of the distribution $P(\Phi)$ is dependent on the neurons being equal or different. In Fig. 7 we have depicted the distribution of the cyclic relative phase for two neurons which receive different tonic subthreshold currents. As we can observe, in this case the distribution $P(\Phi)$ is asymmetric. This distribution should be compared with that appearing in Fig. 6(d), because they both correspond to the point labeled *d* in the synchronization diagram. This comparison shows that depending on which neuron has its phase delayed with respect to the other the distribution of Φ is rather similar or very different to that of the symmetrical system.

IV. TEMPORAL STRUCTURE OF THE PHASE SWITCHING

The behavior of the coupled HH neurons studied in this paper can lead to spike trains with different temporal structures. For values of the coupling parameter near the line $M-B$ the firing is continuous. However, near the onset of spiking regime, the structure of the spike train fired for the neurons depends on the particular choice of the parameters. As we can observe in Figs. 8(a) and 8(b), both neurons can emit bursts of spikes separated for long periods of small oscillations around their resting potentials. During the time course of these bursts, the relative phase performs a number of sudden changes, thus giving rise to a rather complex temporal evolution of the function $\psi(t)$. As we approach the region 2, both the frequency of bursting and the number of spikes per burst decrease, thus announcing the proximity of the silent region. During the intervals between two successive bursts the phase of each neuron remains almost constant due to the large value of $t_{n+1}-t_n$ in Eq. (11). As a consequence, during these interburst periods the relative phase takes values $\psi\approx2n\pi$ with $n=0,1,\ldots,$ and so, only contributions to $P(\Phi\approx0)$ and $P(\Phi\approx2\pi)$ are made. In dynamical regimes with long interburst periods, these extreme values of the cyclic relative phase can correspond to relative maxima of the distribution $P(\Phi)$, as is shown in panels (b), (c), (d), (e), and (f) of Fig. 6.

Starting from the dynamical evolution of ψ in the phase-switching regime, we have obtained a new point process

$$w(t)=\sum_{k=1}^{M}\delta(t-t_k), \tag{14}$$

where a given temporal sequence $\{t_k;k=1,2,\ldots,M\}$ corresponds to the successive times at which a realization of the cyclic relative phase crosses the value $\psi=0$ (switching times). The introduction of this point process allows us to study the temporal structure corresponding to the bistable dynamics of the relative phase founded in the region close to the line $M-B$, which has been described above. This structure can be characterized at a first level by the distribution of switching times. There are only two possible consecutive time-interval sequences available to a two-state system, as shown in Fig. 9. The intervals T_k measure the escape times from the neighborhood of the upper value of the relative phase. On the other hand, the sequence $\{\tau_k\}$ corresponds to the intervals between successive jumps from states around one of the attractors to the other one.

In Fig. 10 we present two histograms characterizing the random behavior of these two different time intervals for the stochastic two-state dynamics of the relative phase ψ. Both histograms show a rapid increase in the number of events as the sizes of the intervals increase, followed by a maximum and a slow decaying tail extending to very long intervals. In a number of cases no phase jumps were detected in the course of stochastic realizations lasting 50 s. The mean in-

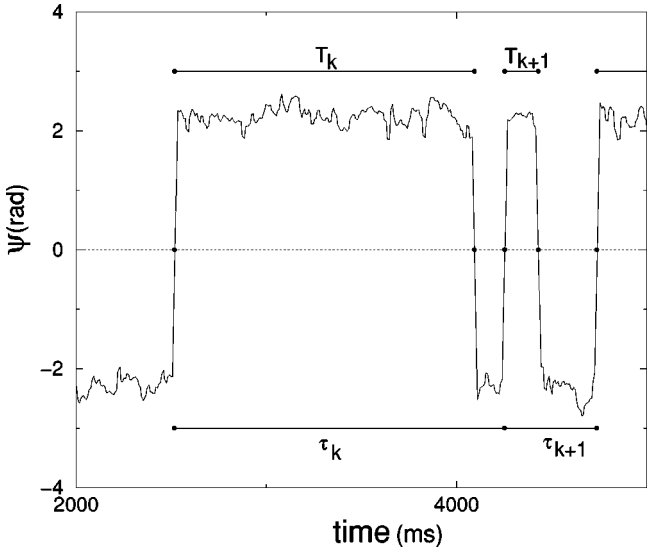

FIG. 9. An example showing the two possible sequences of consecutive time intervals available from the two-state evolution of the relative phase ψ.

tervals obtained were $\langle T\rangle = 726.1$ ms and $\langle \tau\rangle = 1417.8$ ms, suggesting that both quantities are connected by

$$\langle \tau\rangle = 2\langle T\rangle. \tag{15}$$

This relationship in turn suggests that the switching probability is symmetrical. In fact, the structure of these histograms agrees with our previous characterization of the two-state dynamics of the relative phase close to the $M-B$ line as the randomly forced evolution of ψ in an symmetrical bistable potential $U_{eff}(\psi)$.

Given the structure of the above mentioned histograms it is tempting to explore the behavior of the relative phase under the action of a forcing term in order to ascertain the possibility of controlling the switching times by applying external sinusoidal currents to both neurons. Some years ago, Longtin and co-workers characterized SR in bistable systems by means of the multi-modal character of the first passage time distribution function of a particle moving in a double well potential [29] and a huge amount of work has been devoted since then to explore further this idea [30,31]. Notice, however that, unlike what happens in the usual setting of SR, in the present case the variable that performs the well-to-well switchings does not appear explicitly in the Langevin equations of the system. It is not *a priori* obvious that an additive signal acting on the voltage variables could induce such phase switchings.

Let us consider the simultaneous and symmetric forcing of both neurons by an external sinusoidal signal of amplitude A and frequency ω_s acting on the respective voltage equations. In this case, the terms $I_{1(2)}$ appearing in Eq. (9) will be written as

$$I_{1(2)} = I_0 + A\cos\omega_s t, \tag{16}$$

where $I_0 = 6.0\ \mu\mathrm{A/cm}^2$. In Fig. 11 we present some results obtained by integrating the resulting set of stochastic differential equations for a value of the amplitude of the forcing $A = 1.5\ \mu\mathrm{A/cm}^2$. This signal is subthreshold so that in the absence of noise it is unable to excite the firing of the neurons. Also, we have chosen a frequency $\omega_s = 1.25$ Hz which is smaller than the inverse of the mean switching interval in absence of forcing. In the upper panel, a single trajectory for the cyclic relative phase Φ is depicted jointly with a sinusoidal function of period $T_s = 2\pi/\omega_s$ (dashed line). This function provides a useful background to analyze the timing of the phase switching processes. As we can observe, in spite of the very complex behavior of Φ, the sudden jumps from one attractor to the other seem to occur with greater probability at a given phase of the external signal. This statistical locking to the phase of the external signal is demonstrated clearly in the lower panel of Fig. 11, where the (unnormalized) histogram of switching times is depicted. Note the periodic character of this histogram with rather broad maxima separated by time intervals that are equal to the period of the forcing signal $T_s = 5\times 10^3$ ms. Notice also that, in spite of the rather high variability of the time intervals that elapse between successive switchings, these maxima are clearly defined. In fact, they are located at the successive minima of

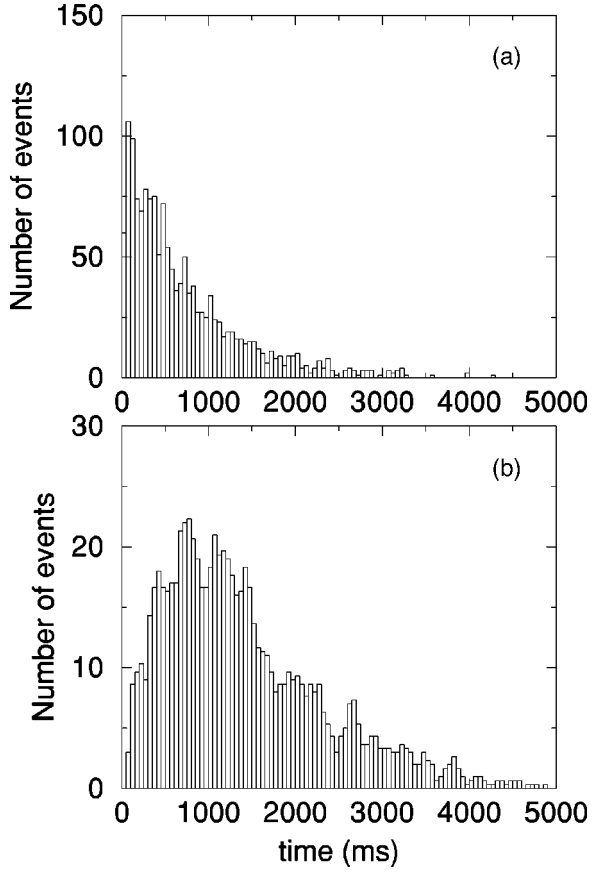

FIG. 10. In panel (a), the histogram of residence times of ψ in one of its attractors is depicted for $\epsilon = 0.07$ and $D = 2\times 10^{-5}$. These values correspond to a random two-state dynamics similar to the one leading to the distribution depicted in panel (a) of Fig. 6. In panel (b), the histogram of intervals between successive jumps from one of the attractors to the other is presented for the same parameters' values.

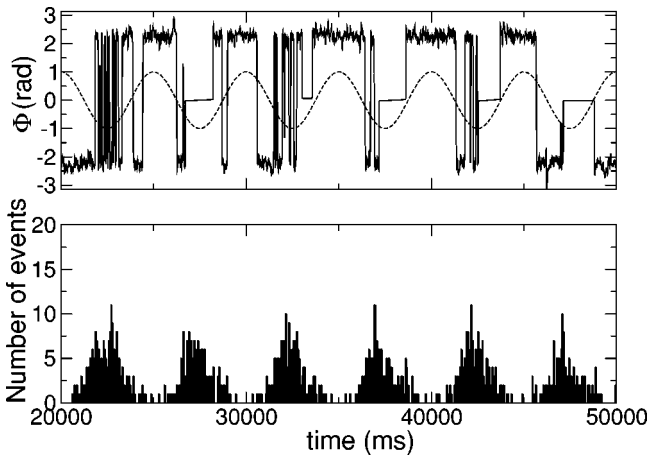

FIG. 11. The timing of phase switchings under external forcing. In the upper panel one stochastic trajectory is depicted to show the behavior of the cyclic relative phase Φ under the action of an external forcing of amplitude $A=1.5\ \mu\mathrm{A/cm}^2$ and period $T_s=5$ s. A graph of a sinusoidal function with the same period and initial phase as the forcing signal is shown by using a dashed line. As we can observe, the successive switching processes occur mainly around a given phase of the external forcing. In the lower panel, a (unnormalized) histogram showing the statistics of the switching times is shown. To construct it, we have used 50 stochastic trajectories, each one lasting 50 s. The model parameters were $\epsilon=0.07$ and $D=2\times10^{-5}$.

the external forcing signal and each one of them is separated from those in its immediate neigborhood by time intervals where very few phase jumps are allowed. Similar results have been obtained for a smaller forcing amplitude ($A=0.75\ \mu\mathrm{A/cm}^2$). However, the use of a greater signal amplitude ($A=2.0\ \mu\mathrm{A/cm}^2$) still locks the cyclic relative phase Φ to the external forcing, but usually the relative phase ψ grows without limit as time increases. It is worth to notice that this is not the case when smaller amplitudes are used (for example, $A=1.5\ \mu\mathrm{A/cm}^2$, corresponding to Fig. 11, or $A=0.75\ \mu\mathrm{A/cm}^2$). For these amplitude values, besides the fact that Φ is statistically locked to the phase of the external forcing, the relative phase ψ always switches between two attractors that remain fixed in time. In summary, it could be said that the pattern of phase switchings transduces the external signal, the quality of this transduction being measured by the width of each peak of the histogram.

V. CONCLUSIONS

By using a realistic neuron model we have shown that both coupling and internal conductance noise could play complementary roles in the emergence of synchronous neural activity. We have studied a system of two diffusively coupled Hodgkin-Huxley neurons in a regime where the deterministic dynamics leads to a nonoscillatory state and we have investigated the role of coupling once the existence of internal noise guarantees the production of spikes by each neuron. For neurons in the strong coupling region a state of statistical out-of-phase synchronization is reached if the noise level is small enough. In this state, the distribution of the cyclic relative phase between neurons peaks around π. As the noise level is increased and the coupling strength is not too strong, this phase-locked evolution is lost and the relative phase can perform a rather complex dynamics characterized by the existence of several attractors. For some combination of coupling and noise the two-state dynamics of the relative phase gives rise to the switching of this quantity between two symmetrical and equiprobable attractors. In this regime, the coupling is strong enough to lock the relative phase near a given value but the noise is able to exchange the role of both neurons from time to time.

In this bistable regime, the simultaneous forcing of both neurons by the same sinusoidal signal can induce the locking of the switching times of the relative phase to the period of the forcing. Thus, the cooperative action of coupling and noise allows the transduction of the external signal by the pattern of phase switchings. In this context, the role of conductance fluctuations is twofold because, on the one hand, for subthreshold signals it is just the noise that allows each neuron to fire so that the transduction process would not take place in its absence. On the other hand, it is clear that intrinsic noise is the origin of the lack of precision in the transduction process. A detailed analysis of this phenomenon will be published elsewhere.

ACKNOWLEDGMENTS

J.M.C. acknowledges the Dirección General de Investigación Científica y Técnica (DGICYT) of Spain for support (Project No. BFM2002-03822). J.P.B. acknowledges support from the Spanish Ministry of Science and Technology under Project No. BFM2000-0967.

[1] J. Kurths, A. Pikovsky, and M. Rosenblum, *Synchronization, A Universal Concept in Nonlinear Science* (Cambridge University Press, Cambridge, 2001).
[2] A. Scott, *Neuroscience: A Mathematical Primer* (Springer-Verlag, New York, 2002).
[3] H.D.I. Abarbanel, M.I. Rabinovich, R. Selverson, M.V. Bazhenov, R. Huerta, M.M. Sushchik, and L.L. Rubchinskii, Usp. Fiz. Nauk **166**, 363 (1996) [Phys. Usp. **39**, 337 (1996)].
[4] Y. Kuramoto, Physica A **106**, 128 (1981).
[5] Y. Kuramoto and I.J. Nishikawa, J. Stat. Phys. **49**, 569 (1987).
[6] L.L. Bonilla, J.M. Casado, and M. Morillo, J. Stat. Phys. **48**, 571 (1987).
[7] H. Daido, Phys. Rev. Lett. **61**, 231 (1988); S.H. Strogatz and R.E. Mirollo, Physica D **31**, 143 (1988).
[8] C. Kurrer and K. Schulten, Physica D **50**, 311 (1991).
[9] A. Sherman and J. Rinzel, Proc. Natl. Acad. Sci. U.S.A. **89**, 2471 (1992).
[10] C.V. Vreeswijk, L.F. Abbott, and G.B. Ermentrout, J. Comput. Neurosci. **1**, 313 (1994).
[11] D. Hansel, G. Mato, and C. Meunier, Europhys. Lett. **23**, 367

(1993); D. Hansel, G. Mato, Physica A **200**, 662 (1993).
[12] S.K. Han, C. Kurrer, and Y. Kuramoto, Phys. Rev. Lett. **75**, 3190 (1995).
[13] C. Morris and H. Lecar, Biophys. J. **35**, 193 (1981).
[14] A.L. Hodgkin and A.F. Huxley, J. Physiol. (London) **117**, 500 (1952).
[15] R. L. Stratonovich, *Topics in the Theory of Random Noise* (Gordon and Breach, New York, 1981).
[16] H. Treutlein and K. Schulten, Eur. Biophys. J. **13**, 355 (1985).
[17] S. Tanabe and K. Pakdaman, Phys. Rev. E **63**, 031911 (2001).
[18] C. Kurrer and K. Schulten, Phys. Rev. E **51**, 6213 (1995).
[19] See, for example, *Single-Channel Recording*, 2nd ed. edited by B. Sackmann and E. Neher (Plenum Press, New York, 1995).
[20] L.J. DeFelice and A. Isaac, J. Stat. Phys. **70**, 339 (1992).
[21] C. Chow and J. White, Biophys. J. **71**, 3013 (1996).
[22] R.F. Fox and Y. Lu, Phys. Rev. E **49**, 3421 (1994).
[23] S. Lee, A. Neiman, and A. Kim, Phys. Rev. E **57**, 3292 (1998).
[24] S. Tanabe, S. Sato, and K. Pakdaman, Phys. Rev. E **60**, 7235 (1999).
[25] A.F. Strassberg and L.J. DeFelice, Neural Comput. **5**, 843 (1993).
[26] See, for example, P. Glendinning, *Stability, Instability and Chaos: an Introduction to the Theory of Nonlinear Differential Equations* (Cambridge University Press, Cambridge, 1994).
[27] J.M. Casado, Phys. Lett. A **310**, 400 (2003).
[28] H.S. Greenside and E. Helfand, Bell Syst. Tech. J. **60**, 1927 (1981).
[29] A. Longtin, A. Bulsara, and F. Moss, Phys. Rev. Lett. **67**, 656 (1991).
[30] L. Gammaitoni, P. Hänggi, P. Jung, and F. Marchesoni, Rev. Mod. Phys. **70**, 223 (1998).
[31] V. Anishchenko, A. Neiman, F. Moss, and L. Schimansky-Geier, Usp. Fiz. Nauk. **169**, 7 (1999) [Phys. Usp. **42**, 7 (1999)].